PHYSICAL REVIEW A VOLUME 25, NUMBER 2 FEBRUARY 1982

Cluster expansion for the electric microfield distribution in a plasma

C. A. Iglesias and C. F. Hooper, Jr.
Department of Physics, University of Florida, Gainesville, Florida 32611
(Received 17 August 1981)

This paper employs a hybrid virial—Debye-chain cluster expansion to reinterpret a collective-coordinate calculation of electric microfield distributions in a plasma. A numerical evaluation of corrections previously neglected is presented. Comparisons with Monte Carlo and molecular-dynamics results are included.

I. INTRODUCTION

The purpose of this paper is to reinterpret the electric microfield distribution calculations developed previously by Hooper,[1] hereafter referred to as I. We will show that the method employed in I is equivalent to a combined virial-Debye expansion similar to that developed by Mayer.[2]

The reinterpretation will start by expressing the high-frequency component electric microfield distribution, due to a one-component plasma, in a cluster expansion similar to the classical expansions of Ursell and Mayer.[3] Then, a split[1] in the central interactions is introduced and an infinite class of terms summed to obtain the results in I. We stress that although similar in technique, the cluster expansion presented here is different from those of previous developments.[1,4] Corrections to I which result from retaining additional correlations will be presented.

The system that we deal with consists of N-charged particles immersed in a uniform neutralizing background. In addition, when treating the problem of the electric field distribution at a charged point, a "zeroth" particle must be included. The $N+1$ particles interact through the Coulomb interaction. The total system is assumed to be in thermal equilibrium and macroscopically neutral.

Section II of this paper deals with the development of the formalism. The corrections to the results in I are discussed in Sec. III with the numerical results given in Sec. IV. Final conclusions are discussed in the fifth and final section.

II. FORMALISM

Define $Q(\vec{\epsilon})$ as the probability of finding an electric field $\vec{\epsilon}$, at a singly charged point located at $\vec{r}_0$, due to N-charged particles moving in a uniform neutralizing background and contained in a volume Ω. Then, if Z represents the configurational partition function of the $N+1$ particle system, we may write

$$Q(\vec{\epsilon})=Z^{-1}\int\cdots\int d\vec{r}_0 d\vec{r}_1\cdots d\vec{r}_N e^{-\beta V}\times\delta(\vec{\epsilon}-\vec{E}) , \tag{1}$$

where $\vec{r}_j$ represents the coordinate of the jth particle, $\beta=(kT)^{-1}$, V the potential energy of the system, and $\vec{E}$ is the electric field at $\vec{r}_0$ due to the N-charged particles in a given coordinate configuration.

The potential energy of the system V is expressed as

$$V=\sum_{0=i<j}^{N} e^2/r_{ij}+V_B , \tag{2}$$

where V_B represents the contributions to the potential energy due to the neutralizing background.

An expression for V in terms of a Fourier expansion results in

$$V=\frac{4\pi e^2}{\Omega}\sum_{k\neq 0}\sum_{0=i<j}^{N} e^{-i\vec{k}\cdot\vec{r}_{ij}}/k^2 , \tag{3}$$

where the exclusion of the $\vec{k}=0$ term in Eq. (3) accounts for the neutralizing background.[5]

Assuming that our system is isotropic we may rewrite[5] Eq. (1) as

$$P(\epsilon)=2\pi^{-1}\epsilon\int_0^\infty dl\, lT(l)\sin(\epsilon l) , \tag{4}$$

where $P(\epsilon)$ is related to $Q(\vec{\epsilon})$ by the relation

$$4\pi Q(\vec{\epsilon})\epsilon^2 d\epsilon=P(\epsilon)d\epsilon ; \tag{5}$$

$T(l)$ is defined by

$$T(l)\equiv Z(l)/Z , \tag{6}$$

$$Z(l)\equiv\int\cdots\int d\vec{r}_0 d\vec{r}_1\cdots d\vec{r}_N e^{-\beta V(l)}\,, \quad (7)$$

$$V(l)\equiv\sum_{0=i<j}^{N} v_{ij}(l)=\sum_{0=i<j}^{N}\left[1-\frac{i\vec{l}\cdot\vec{\nabla}_0}{e\beta}\right]v_{ij}\,, \quad (8)$$

where $v_{ij}=e^2/r_{ij}$ and $\vec{\nabla}_0$ is the gradient with respect to $\vec{r}_0$.

The function $Z(l)$ has the form of a configurational partition function with the potential energy of the system $V(l)$, defined in Eq. (8). We proceed to calculate numerator and denominator of Eq. (6) using the classical cluster expansions for configurational partition functions which were developed by Ursell and Mayer.[3]

Again noting that the numerator $Z(l)$ has the form of a configurational partition function, we write it in the form of a Helmholtz free energy, $F(l)$:

$$Z(l)=e^{-\beta F(l)}\,, \quad (9)$$

$F(l)$ given by

$$-\beta F(l)=\Omega A(\rho,l)\,. \quad (10)$$

Now the quantity A can be expressed in terms of a cluster expansion,[3]

$$A(\rho,l)=\sum_{n=2}^{N}\frac{\rho^n}{n!}\int\cdots\int R(n,l)\prod_{j}^{n}d\vec{r}_j\,. \quad (11)$$

Here, $R(n,l)$ is the sum of all products of f-Mayer functions in which every particle in n is independently connected to every other particle in n. The f-Mayer functions are defined as

$$f_{ij}(l)=(e^{-\beta v_{ij}(l)}-1)\,, \quad (12)$$

where n represents the set of $n=n_0+n_i$ particles,

$$n!=n_0!n_i!\,,$$

$$\rho^n=\rho_o^{n_0}\rho^{n_i}\,;\rho_0=\Omega^{-1}\,,\rho=N/\Omega\,, \quad (13)$$

$\int\cdots\int\prod_j^n d\vec{r}_j$ represents the integrations over set of n particles; n_0 and n_i are the number of zeroth particles, here equal to 0 or 1, and N-charged particles in the cluster $R(n,l)$, respectively.

The clusters in the expansion of $A(\rho,l)$ are of two types: (1) clusters which do not contain the zeroth particle, $n_0=0$; (2) clusters which do contain the zeroth particle, $n_0=1$. If $A_1(\rho)$ and $A_2(\rho,l)$ denote the contributions from all type (1) and (2) clusters, respectively, then

$$Z(l)=\exp[\Omega A_1(\rho)+\Omega A_2(\rho,l)]\,. \quad (14)$$

A similar procedure can be applied to $Z=Z(l=0)$, with the result

$$Z(l=0)=\exp[\Omega A_1(\rho)+\Omega A_2(\rho,0)]\,. \quad (15)$$

The term $A_1(\rho)$ is independent of l; in fact, $\exp[\Omega A_1(\rho)]$ is the configurational partition function for the plasma without the zeroth particle.

Substituting Eq. (14) and Eq. (15) in Eq. (6) allows us to write

$$T(l)=\exp[\Omega(A_2(\rho,l)-A_2(\rho,0))]\,. \quad (16)$$

That is, all clusters not involving the zeroth particle cancel exactly in Eq. (16).

A graphical representation[3] of some of the terms appearing in A_2 is shown in Fig. 1; a black vertex represents one of the N-charged particles, a white vertex the zeroth particle. Each f-Mayer function is represented by a heavy-solid line connecting two vertices.

As in I, we conjecture that quantitative features of the microfield distribution will be more sensitive to central than to noncentral interactions. A central interaction involves the zeroth particle and one of the N-charged particles; a noncentral interaction involves any pair of N-charged particles. Based on this conjecture, the details of the central interactions are treated with greater care. Therefore, we split the central interactions into long- and short-range contributions. The long-range central and all of the noncentral Coulomb interactions we treat in a Debye-chain[6] expansion. After the long-range contributions are renormalized, all the remaining short-range "interactions" are treated by means of a virial expansion. From an examination of the formalism it is clear that the two expansions are not independent but involve a hybrid (virial-Debye) cluster expansion. It must be emphasized that the conjecture discussed above is based on a plausibility argument, which is justified by results.[1,7,8] To carry out this procedure, we first set

$$v_{0j}=u_{0j}+w_{0j}\,, \quad (17)$$

where

$$w_{0j}=(e^2/r)e^{-\alpha r_{0j}/\lambda}\,. \quad (18)$$

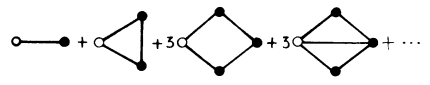

FIG. 1. Graphical representation of A_2. A black vertex represents an ion, a white vertex the zeroth particle. Each f-Mayer function is represented by a heavy-solid line connecting two vertices.

α is an arbitrary, real, positive parameter which will be independently determined, and λ is the Debye length,

$$\lambda=(4\pi e^2\rho\beta)^{-1/2} . \tag{19}$$

Substitute Eq. (17) into the expression for the f-Mayer functions, Eq. (12). This yields a result similar to one used by Ref. 2, but with the difference that in the present paper only central interactions are split

$$f_{ij}(l)=\begin{cases}(e^{-\beta v_{ij}}-1) & i,j\neq 0\\ \chi_j(l)+[1+\chi_j(l)]\sum_{n=1}^{\infty}[-\beta u_{0j}(l)]^n/n!, & i=0,\ j\neq 0\end{cases} \tag{20}$$

where

$$\chi_j(l)=(e^{-\beta w_{0j}(l)}-1) . \tag{21}$$

with the aid of Eq. (20) we may further separate the products in $R(\rho,l)$ into sums of products involving the f function, χ function, and $(-\beta u)^n/n!$ functions represented by heavy-solid lines, light-solid lines, and n-dashed lines, respectively. Clearly, there can be at most one f or χ bond directly connecting two vertices. The result of splitting the central interactions is shown graphically for some two- and three-particle clusters in Fig. 2(a). The two $(-\beta u)$-bonds with the triple dot in between represent the sum of graphs with all possible number of $(-\beta u)$-bonds as shown in Fig. 2(b).

In order to perform a Debye-chain expansion on the long-range central and noncentral interactions, we expand the noncentral f-Mayer functions in powers of $(-\beta v)$. With the decomposition of the f functions into powers of $(-\beta v)$ functions we can sum simple chains of $(-\beta u)$- and $(-\beta v)$-bonds as shown in Fig. (3). Two types of chains are possible: The first has the zeroth particle and one perturbing ion for endpoints while the second has two ions for endpoints. It is understood that the two vertices at the endpoints of Fig. (3) are, in general, part of a more complicated graph. Hence, we are summing all graphs which are the same except for the one sum of interactions displayed. The intermediate ions in Fig. (3) do not interact with any particles except as explicitly shown in the figure. The final form for A_2 is an infinite series of integrals involving products of the functions χ, u^s, and v^s; u^s and v^s are defined graphically in Fig. (3) and evaluated in Appendix A. There is the restriction that no simple chains in the effective interactions u^s and v^s appear in A_2 because such a chain is, in effect, a simple chain in u and v interactions which have been already included in the summations. The new cluster expansion for A_2 is given by

$$\Omega A_2(\rho,l)=\ln T_0(l)+\sum_{n=1}^{\infty}\frac{\rho^n}{n!}h_n(l) , \tag{22}$$

where $\ln T_0(l)$ is the contribution from the ring graphs presented graphically in Fig. 4(a), and h_n is the set of all $n+1$ particle clusters, excluding ring graphs, involving products of the functions χ, u^s, and v^s as described above and presented graphically in Figs. 4(b) and 4(c) for $n=1$ and 2.

In Fig. (4) we have separated the graphs for $n=1$ and 2 into the subsets (b1), (b2) and (c1), (c2). The separation is employed since it can be shown that only the graphs shown in (b1) and (c1) are included in I. There, only the first term in the Gram Charlier[9] expansion series for the Jacobian

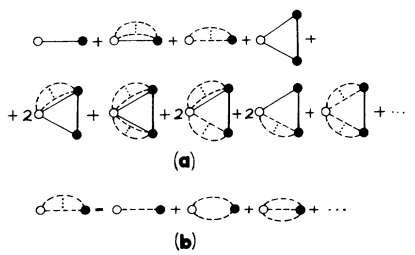

FIG. 2. Some two- and three-particle clusters in A_2 after the splitting of the central interactions. The f-Mayer, χ, and $(-\beta u)^n/n!$ functions are represented by heavy-solid lines, light-solid lines, and n-dashed lines, respectively.

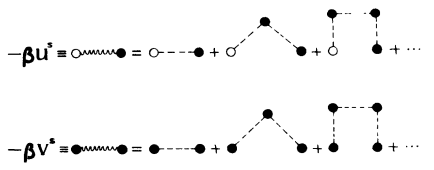

FIG. 3. Effective interactions u^s and v^s.

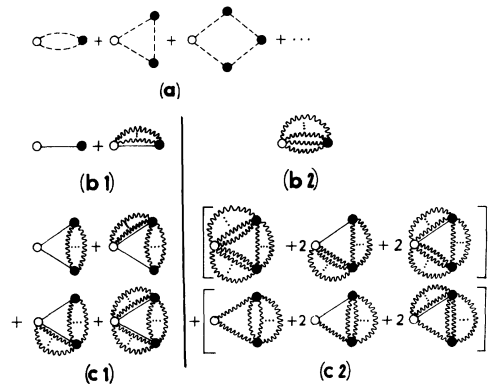

FIG. 4. Contributions to A_2 up to $n=2$ of Eq. (22). (a) The ring graphs. (b1) and (c1) are the graphs included in the Jacobian approximation in I. (b2) and (c2) are the neglected terms in I. The triple dot has the same meaning here as in Fig. 2, except now it refers to $(-\beta v^s)$- or $(-\beta u^s)$-bonds. Note that the noncentral bonds in the second bracket of (c2) have a minimum of two $(-\beta v^s)$-bonds. The graph in (b2) has a minimum of three $(-\beta u^s)$-bonds.

of the collective coordinate transformation is retained. We will show that the graphs (b2) and (c2) are neglected by such an approximation.

Splitting up the potential appearing in $Z(l=0)$ in the same manner as previously described in treating $Z(l)$, we are able to carry out a similar expansion program with the result

$$\Omega A_2(\rho,0)=\ln T_0(0)+\sum_{n=1}^{\infty}\frac{\rho^n}{n!}h_n(0)\ . \tag{23}$$

The graphs representing the terms in Eq. (23) are topologically equivalent to those in Eq. (22) but with l set equal to zero.

Combining Eqs. (16), (22), and (23) gives the following result for $T(l)$:

$$T(l)=[T_0(l)/T_0(0)]\times\exp\left[\sum_{n=1}^{\infty}\frac{\rho^n}{n!}[h_n(l)-h_n(0)]\right]\ . \tag{24}$$

Now consider the individual terms appearing in Eq. (24). In Appendix B we show that the first term, $T_o(l)/T_0(0)$, can be written as

$$T_0(l)/T_0(0)=\exp(-\gamma L^2)\ . \tag{25}$$

In Eq. (25),

$$L=l\epsilon_0,\quad \gamma=a\alpha^3/4(\alpha+1)^2,\quad a=r_0/\lambda$$

and

$$\epsilon_0=e/r_0^2;$$

r_0 is the ion sphere radius defined by the expression

$$\frac{4\pi}{3}r_0^3\rho=1\ . \tag{26}$$

Next, we consider the factors resulting from terms in the series exponent. For $n=1$, and considering only terms shown graphically in Fig. (4b1), we write

$$\begin{aligned}I_1^{(1)}(l)&=\rho[h_1^{(1)}(l)-h_1^{(1)}(0)] \\ &=\rho\int d\vec{r}_{10}[\chi_1(l)Q_1(l)-\chi_1(0)Q_1(0)] \\ &=3\int_0^{\infty}dx\,x^2\left[e^{F(x)}\left[\frac{\sin[LG(x)]}{LG(x)}-1\right]\right. \\ &\quad\left.-e^{s(x)}\left[\frac{\sin[Lq(x)]}{Lq(x)}-1\right]\right],\end{aligned} \tag{27}$$

where the angular integrations have been done. The functions in the second equality are defined by

$$Q_1(l)=\exp[-\beta u^s(\vec{r}_{10},l)]\ , \tag{28}$$

$$u^s(\vec{r}_{10},l)=\left[1-\frac{i\vec{l}}{e\beta}\cdot\vec{\nabla}_0\right]u^s(r_{10})\ . \tag{29}$$

The functions in the third equality are defined in Sec. III: Eqs. (35), (36), (38), and (39).

For the second term in the series, $n=2$, we use the graphs in Fig. (4c1) to write

$$\begin{aligned}I_2^{(1)}(l)&=\frac{\rho^2}{2}[h_2^{(1)}(l)-h_2^{(1)}(0)] \\ &=\frac{\rho^2}{2}\int\int d\vec{r}_{10}d\vec{r}_{20}[\chi_1(l)\chi_2(l)Q_1(l)Q_2(l)-\chi_1(0)\chi_2(0)Q_1(0)Q_2(0)](e^{-\beta v_{12}^s}-1)\ .\end{aligned} \tag{30}$$

Thus, the contributions to $T(l)$ from Figs. 4(a), 4(b1), and 4(c1) are given by

$$T^{(1)}(l)=\exp[-\gamma L^2+I_1^{(1)}(l)+I_2^{(1)}(l)]\ . \tag{31}$$

The results in Eqs. (25)–(31) are identical to those in I for $T(l)$ as given in Eqs. (25)–(35) of I.

III. CORRECTIONS

In Sec. II we expressed the microfield distribution function in terms of a cluster expansion where the long-range interactions are treated in a Debye-chain expansion and the short-range interactions in a virial expansion. The two are not independent but involve a hybrid virial Debye-chain cluster expansion with the long-range collective effects of the Debye chains modifying the short-range virial expansion.

As mentioned earlier, the graphs in Figs. 4(b2) and 4(c2) are not included in the results of Eq. (31). The neglected terms can be interpreted as correlations between the collective coordinates introduced in I. In this section we will evaluate these contributions to $T(l)$ for $n=1$ and 2 in Eq. (24).

The corrections to $I_1(l)$, shown graphically in Fig. 4(b2), is given by

$$\begin{aligned} I_1^{(2)}(l)&=\rho[h_1^{(2)}(l)-h_1^{(2)}(0)] \\ &=\rho\int d\vec{r}_1(\{e^{-\beta u^s(\vec{r}_1,l)}-\tfrac{1}{2}[\beta u^s(\vec{r}_1,l)]^2 \\ &\quad +\beta u^s(\vec{r}_1,l)-1\}-\{e^{-\beta u^s(r_1)}-\tfrac{1}{2}[\beta u^s(r_1)]^2+\beta u^s(r_1)-1\}) . \end{aligned} \tag{32}$$

Performing the angular integrations we get

$$I_1^{(2)}(l)=3\int_0^\infty dx\,x^2\left[e^{s(x)}\left[\frac{\sin[Lq(x)]}{Lq(x)}-1\right]+\frac{L^2q^2(x)}{6}\right] . \tag{33}$$

The functions that appear in the integrand are defined as follows:

$$x=r/r_0 , \tag{34}$$

$$s(x)=\frac{\alpha^2}{1-\alpha^2}\left[\frac{a^2}{3x}\right](e^{-ax}-e^{-\alpha ax}) , \tag{35}$$

$$q(x)=\frac{\alpha^2}{1-\alpha^2}\left[\frac{1}{x^2}(e^{-\alpha ax}-e^{-ax})-\frac{a}{x}(e^{-ax}-\alpha e^{-\alpha ax})\right] . \tag{36}$$

Combining Eqs. (27) and (33) we find that

$$I_1(l)=3\int_0^\infty dx\,x^2\left[e^{F(x)}\left[\frac{\sin[LG(x)]}{LG(x)}-1\right]+\frac{L^2q^2(x)}{6}\right] , \tag{37}$$

with

$$F(x)=\frac{1}{1-\alpha^2}\left[\frac{a^2}{3x}\right](\alpha^2e^{-ax}-e^{-\alpha ax}) , \tag{38}$$

$$G(x)=\frac{1}{1-\alpha^2}\left[\frac{1}{x^2}(e^{-\alpha ax}-\alpha^2e^{-ax})+\frac{a}{x}(\alpha e^{-\alpha ax}-\alpha^2e^{-ax})\right] . \tag{39}$$

Before evaluating the contributions from the graphs in Fig. 4(c) we note that the sum of three particle clusters is a small correction[1] to $T(l)$. Hence, we only consider graphs with the lowest nonvanishing number of $(-\beta v^s)$-bonds connecting particles 1 and 2. With this simplification the graphs in Fig. 4(c) will be of two types; graphs with one $(-\beta v^s)$-bond, and graphs with two $(-\beta v^s)$-bonds.

The contribution to $T(l)$ from graphs with one $(-\beta v^s)$-bond is given by

$$I_2^{(1)}(l)=\frac{-\beta\rho^2}{2}\int d\vec{r}_1d\vec{r}_2v^s(r_{12})[\chi_1(l)\chi_2(l)e^{-\beta u^s(\vec{r}_1,l)}e^{-\beta u^s(\vec{r}_2,l)}-\chi_1(0)\chi_2(0)e^{-\beta u^s(r_1)}e^{-\beta u^s(r_2)}] , \tag{40}$$

$$I_2^{(2,1)}(l)=\frac{-\beta\rho^2}{2}\int d\vec{r}_1 d\vec{r}_2 v^s(r_{12})(\{[e^{-\beta u^s(\vec{r}_1,l)}+\beta u^s(\vec{r}_1,l)-1][e^{-\beta u^s(\vec{r}_2,l)}+\beta u^s(\vec{r}_2,l)-1]$$
$$-[e^{-\beta u^s(r_1)}+\beta u^s(r_1)-1][e^{-\beta u^s(r_2)}+\beta u^s(r_2)-1]\}$$
$$+2\{[e^{-\beta u^s(\vec{r}_1,l)}+\beta u^s(\vec{r}_1,l)-1]e^{-\beta u^s(\vec{r}_2,l)}\chi_2(l)$$
$$-[e^{-\beta u^s(r_1)}+\beta u^s(r_1)-1]e^{-\beta u^s(r_2)}\chi_2(0)\})\,. \tag{41}$$

$I_2^{(1)}(l)$ corresponds to the graphs in Fig. 4(c1) and $I_2^{(2,1)}(l)$ to the graphs in the first bracket of Fig. 4(c2).

The integrands in Eqs. (40) and (41) are a product of functions of $(\vec{r}_1,l)$ and $(\vec{r}_2,l)$ with the exception of the r_{12} coupling term in $v^s(r_{12})$. In order to uncouple the r_1, r_2 dependence, we expand $v^s(r_{12})$ in sherical harmonics[10]:

$$v^s(r_{12})=-\sum_{k=0}^{\infty}(2k+1)v_k^2(r_1,r_2)P_k(\cos\theta_{12})\,, \tag{42}$$

where

$$v_k^s(r_1,r_2)=\frac{a^2}{3}K_{k+1/2}(ax_1)I_{k+1/2}(ax_2)/(x_1x_2)^{1/2}\,, \tag{43}$$

and $x_j=r_j/r_0$, $x_1>x_2$, and $k=0, 1, 2,\ldots$. This method allows Eqs. (40) and (41) to be reduced to a tractable double integral where the angular integrations are readily performed to yield

$$I_2^{(1)}(l)+I_2^{(2,1)}(l)=3a^2\sum_{k=0}^{\infty}\int_0^{\infty}dx_2x_2^{3/2}I_{k+1/2}(ax_2)\int_{x_2}^{\infty}dx_1x_1^{3/2}K_{k+1/2}(ax_1)$$
$$\times(-1)^k(2k+1)[i_k^{(1)}(x_1,x_2)+i_k^{(2,1)}(x_1,x_2)]\,, \tag{44}$$

$$i_k^{(1)}(x_1,x_2)=e^{s(x_1)}e^{s(x_2)}\{[e^{-\beta w(x_1)}j_k(LG(x_1))-j_k(Lq(x_1))][e^{-\beta w(x_2)}j_k(LG(x_2))$$
$$-j_k(Lq(x_2))]-\delta_{k,0}\chi_1(0)\chi_2(0)\}\,, \tag{45}$$

$$i_k^{(2,1)}(x_1,x_2)=[e^{s(x_2)}(2e^{-\beta w(x_2)}j_k(LG(x_2))-j_k(Lq(x_2)))-\delta_{k,0}(1+s(x_2))][e^{s(x_1)}j_k(Lq(x_1))-\delta_{k,0}]$$
$$-\delta_{k,0}[(e^{s(x_1)}-1)\{e^{s(x_2)}(2e^{-\beta w(x_2)}-1)-[1+s(x_2)]\}$$
$$+s(x_1)e^{s(x_2)}[2e^{-\beta w(x_2)}(j_0(LG(x_2))-1)-(j_0(Lq(x_2))-1)]]$$
$$-\frac{L}{3}\delta_{k,1}\{q(x_1)e^{s(x_2)}[2e^{-\beta w(x_2)}j_1(LG(x_2))-j_1(Lq(x_2))]$$
$$+q(x_2)[e^{s(x_1)}j_1(Lq(x_1))-Lq(x_1)/3]\}\,. \tag{46}$$

The functions I and K refer to modified Bessel functions of the first and third kind, respectively, while j_k specifies a spherical Bessel function of order k.[11]

The second bracket in Fig. 4(c2) shows the graphs with a minimum of two $(-\beta v^s)$-bonds. Their approximate contribution to $T(l)$ is given by

$$I_2^{(2,2)}(l)=\frac{\rho^2\beta^2}{2}\int d\vec{r}_1 d\vec{r}_2 v^s(r_{12})^2\left[\frac{\beta^2}{2}[u^s(\vec{r}_1,l)u^s(\vec{r}_2,l)-u^s(r_1)u^s(r_2)]\right.$$
$$\left.-\beta[u^s(\vec{r}_1,l)e^{-\beta u^s(\vec{r}_2,l)}\chi_2(l)-u^s(r_1)e^{-\beta u^s(r_2)}\chi_2(0)]\right]\,. \tag{47}$$

The first term in square brackets in Eq. (47) may be evaluated by introducing the Fourier transforms as in Appendix B. Then,

$$\frac{\rho_2\beta^4}{4}\int d\vec{r}_1 d\vec{r}_2 v^s(r_{12})^2[u^s(\vec{r}_1,l)u^s(\vec{r}_2,l)-u^s(r_1)u^s(r_2)]=-\gamma_1 L^2\,,$$
$$\gamma_1=\frac{-a^2\alpha^4}{12(\alpha^2-1)^3}\left[(\alpha^2+1)\ln\left[\frac{3}{2+\alpha}\right]+\frac{(\alpha^2-1)(2\alpha+1)}{3(\alpha+2)}\right]. \tag{48}$$

The term in the second square bracket in Eq. (47) may be reduced to a one-dimensional integral by first integrating over $\vec{r}_1$,

$$\frac{\rho^2\beta^3}{2}\int d\vec{r}_1 d\vec{r}_2 v^s(r_{12})^2[u^s(\vec{r}_1,l)e^{-\beta u^s(\vec{r}_2,l)}\chi_2(l)-u^s(r_1)e^{-\beta u^s(r_2)}\chi_2(0)]$$
$$=\left[\frac{3}{4\pi}\right]\int d\vec{x}_2\{[t(x_2)+iLp(x_2)\cos\theta_2]e^{s(x_2)}(e^{-\beta w(x_2)}e^{iLG(x_2)\cos\theta_2}$$
$$-e^{iLq(x_2)\cos\theta_2})-t(x_2)e^{s(x_2)}\chi_2(0)\}$$
$$=3\int_0^\infty dx\,x^2\left\{t(x)\left[e^{F(x)}\left[\frac{\sin[LG(x)]}{LG(x)}-1\right]-e^{s(x)}\left[\frac{\sin[Lq(x)]}{Lq(x)}-1\right]\right]\right.$$
$$\left.-Lp(x)[e^{F(x)}j_1(LG(x))-e^{s(x)}j_1(Lq(x))]\right\}, \tag{49}$$

where in Eq. (49)

$$t(x)\equiv\frac{-a^5}{36x}\left[\frac{\alpha^2}{\alpha^2-1}\right]\left(e^{ax}E_1(3ax)+e^{ax}[\ln 3-E_1(ax)]\right.$$
$$\left.-\frac{e^{a\alpha x}}{\alpha}E_1[(2+\alpha)ax]-\frac{e^{-a\alpha x}}{\alpha}\left\{\ln\left[\frac{2+\alpha}{2-\alpha}\right]-E_1[(2-\alpha)ax]\right\}\right), \tag{50}$$

$$p(x)\equiv x^{-1}\left(\frac{-a^4}{12}\left[\frac{\alpha^2}{\alpha^2-1}\right]\left\{e^{ax}E_1(3ax)-e^{-ax}[ln 3-E_1(ax)]-e^{a\alpha x}E_1[(2+\alpha)ax]\right.\right.$$
$$\left.\left.+e^{-a\alpha x}\left[\ln\left[\frac{2+\alpha}{2-\alpha}\right]-E_1[(2-\alpha)ax]\right]\right\}-\frac{3t(x)}{a^2}\right). \tag{51}$$

Equations (50) and (51) are only valid for values of α less than 2. The function E_1 is the exponential integral

$$E_1(y)\equiv\int_y^\infty dz\frac{e^{-z}}{z}\quad\text{for } y>0\,. \tag{52}$$

Combining Eqs. (40), (41), and (47) we have

$$I_2(l)=I_2^{(1)}(l)+I_2^{(2,1)}(l)+I_2^{(2,2)}(l)\,. \tag{53}$$

Thus,

$$T(l)\simeq\exp[-\gamma' L^2+I_1(l)+I_2(l)]\,, \tag{54}$$

with $\gamma'=\gamma+\gamma_1$, and $I_1(l)$ is given by Eq. (37) and $I_2(l)$ by Eq. (53). The result in Eq. (54) is used in Eq. (4) to calculate $P(\epsilon)$ at a singly charged point in Sec. IV.

IV. RESULTS

The first step in using and evaluating the present theory is to determine the parameter α. In principle, the expression for $T(l)$ in Eq. (24) is independent of the choice of α. However, in a practical calculation the infinite series appearing in the exponent of Eq. (24) is terminated and $T(l)$ is then no longer independent of the value of α. The procedure for selecting α is discussed in detail in I. Briefly, it involves finding a distinct and extended

range of α values over which the $T(l)$ curve, hence the $P(\epsilon)$ curve, remains stationary. In the stability region, or α plateau, the second term in the series is small and the series rapidly converges.

A justification for the α-selection procedure follows. For a given a, a particular choice of α determines how much of the central interaction is treated by a Debye chain or by a virial expansion. The validity and speed of convergence of such expansions depend on the detailed nature of the interactions treated. A best choice of α will be that which splits the central interactions so as to optimize both expansions, thus giving a rapid convergence of Eq. (24). Then, a small variation of α about the best value should not significantly affect the results provided sufficient terms are retained in the infinite series.

Using this procedure we calculate $P(\epsilon)$ curves and compare them (Sec. III) with the results of I. Figures 5 and 6 show $P(\epsilon)$ curves for $a=1.73$ and $a=2.45$, respectively. From the plots it can be seen that the corrections slightly lower and shift the peaks of the $P(\epsilon)$ curves to higher ϵ values. Although not shown here, the contribution from these corrections become smaller with decreasing values of a. In Fig. 5 we compare our curves with Monte Carlo results[12] and in Fig. 6 with molecular-dynamic results.[13] The agreement for $a=1.73$ is quite good. In this case, there exists a well-defined α plateau.

For $a=2.45$ the α plateau is reduced to essentially an extremum point making the theory sensitive to the particular choice of α. If we proceed and calculate $P(\epsilon)$ with the extrement point as our choice for α, then we obtain results which are not in good agreement with the computer experiments as shown in Fig. (6). The lack of agreement, together with our earlier discussion of the α-selection procedure would indicate the need to retain more terms in the series of Eq. (24) for $a \gtrsim 2.0$.

V. CONCLUSION

We have shown that the previously developed collective coordinate approach to microfield distributions is equivalent to a hybrid virial-Debye expansion. The two expansions are not independent; the long-range collective effects of the Debye chains modify the short-range virial expansion. Hence, the range of validity of this formalism, when applied to systems where particles interact through long-range potentials, exceeds that of theories that use either expansion separately.[14] The hybrid virial-Debye expansion formalism can easily be extended to the low-frequency microfield distributions in a plasma containing multiply charged ions.[8]

Numerical calculations of $P(\epsilon)$ curves including some corrections neglected in I are presented in graphical form. These corrections correspond to correlations between the collective coordinates. Their contribution can be shown to be equivalent to keeping the next term in the Gram Charlier expansion of the Jacobian of the transformation to collective coordinates. Even though the effect of the corrections is small, for $a=2.45$ they improve agreement with the results of computer experiment.

In Eq. (22) we have ordered the terms in the sum by the number of particles in a cluster. We now propose a different ordering based on the splitting of the central interactions. This split separates the central interaction into a strong short-ranged and a weak long-range contribution. The long-range weakly coupled part requires a Debye-chain expansion since these infinite range interactions give rise to collective effects. We treat-

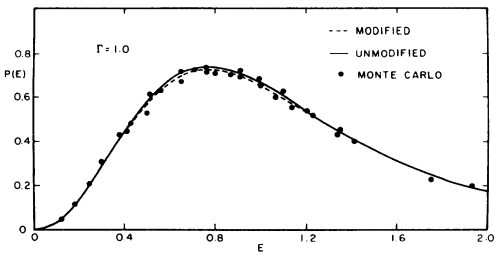

FIG. 5. Comparison of $P(\epsilon)$ curves for $a=1.732$. The unmodified curve refers to the results of I. The modified curve includes the corrections in Sec. III. ϵ is in units of ϵ_0.

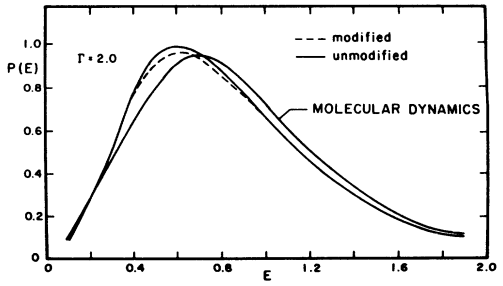

FIG. 6. Comparison of $P(\epsilon)$ curves for $a=2.45$. The unmodified curve refers to the results of I. The modified curve includes the corrections in Sec. III. ϵ is in units of ϵ_0.

ed the strongly coupled part given by the χ bonds and the effective interactions resulting from the summation of Debye chains in a virial expansion. However, instead we may identify a cluster by the number of χ bonds it contains, and by the complexity[11] of the weakly coupled contributions. For example, the lowest-order terms in complexity are the ring graphs,[11] and the simple chains in Fig. (3). A systematic correction procedure in Ref. 15 discusses at length the summation of graphs of higher order in complexity. Therefore, we propose to order the terms in Eq. (24) by the two parameters: χ bonds and complexity of the weakly coupled interactions.

In the preceding discussion we have implicitly assumed that the noncentral interactions constitute a weakly coupled system. This, of course, is only true for value of $a << 2.0$. However, our original conjecture is that the microfield distribution is not very sensitive to the noncentral interactions. In this sense the noncentral interactions can be weakly coupled to the zeroth particle.

From Fig. (4) we see that in this new ordering scheme the graphs in (b2) and (c2) are of zeroth and first order in the strong coupling parameter, the number of χ bonds. These graphs are higher order in complexity of the weakly coupled contributions than the graphs in (a), (b1), and (c1). We see that the graphs in (b2) and (c2) of zeroth and first order in χ bonds are to be grouped with the ring graphs in (a) and the graphs in (b1), respectively.

From our results in Sec. IV, we believe that by including terms containing three χ bonds and lowest order in complexity in the Debye chains we can extend the validity of our results to values of $a \gtrsim 2.0$.

As a final remark, we note the similarity between the hybrid expansion presented here and those developed in Ref. 2 for evaluating the osmotic pressure and the radial distribution function. However, there the short-ranged interactions are due to internal structure of the particles; more importantly the short-ranged contributions are included in the interactions between all pairs of particles whereas in this development they are present only in the central interactions.

Research supported in part by a grant from the Department of Energy, and subcontracts from the Lawrence Livermore Laboratory and Laboratory for Laser Energetics.

APPENDIX A

In this appendix we are concerned with explicit evaluation of the effective interactions, $\beta u^s(\vec{r},l)$, indicated in Fig. (3). The simple chain summation which produces $-\beta u^s(\vec{r},l)$ has the following analytic form:

$$-\beta u^s(\vec{r}_{01},l) = -\beta u(r_{01},l) - \beta \sum_{j=2}^{\infty} (-\beta\rho)^{j-1} \int \cdots \int d\vec{r}_2 \cdots d\vec{r}_j \, u(\vec{r}_{02},l) v(r_{23}) \cdots v(r_{j1})$$

$$= \left[1 - \frac{i\vec{l}\cdot\vec{\nabla}_0}{e\beta}\right] \left[-\beta u(r_{01}) - \beta \sum_{j=2}^{\infty} (-\beta\rho)^{j-1} \int \cdots \int d\vec{r}_2 \cdots d\vec{r}_j \, u(r_{02}) v(r_{23}) \cdots v(r_{j1})\right] . \tag{A1}$$

Introduce the Fourier transforms

$$p(\vec{r}) = \frac{1}{(2\pi)^3} \int d\vec{q} \, e^{i\vec{q}\cdot\vec{r}} p(\vec{q}) , \tag{A2}$$

where $p(\vec{r})$ stands for u, u^s, v, or v^s. Then, using the Faultung (convolution) method obtain for the transform of $u^s(\vec{r}_{10},l)$,

$$u^s(\vec{q},l) = \left[1 - \frac{\vec{l}\cdot\vec{q}}{e\beta}\right] u(q)/\epsilon(q) . \tag{A3}$$

The dielectric response function ϵ and the transform of $u(r)$ and $v(r)$ are defined by

$$\epsilon(q)=1+\rho\beta v(q)\ ,$$
$$u(q)=\frac{4\pi e^2\alpha^2}{q^2[\alpha^2+(\lambda q)^2]}\ , \tag{A4}$$
$$v(q)=\frac{4\pi e^2}{q^2}\ .$$

Similarly, for the noncentral effective interaction,

$$v^s(q)=v(q)/\epsilon(q)\ . \tag{A5}$$

Equations (A3) and (A5) may be inverse transformed to yield

$$u^s(r)=\frac{\alpha^2}{\alpha^2-1}\left[\frac{e^2}{r}\right](e^{-r/\lambda}-e^{-\alpha r/\lambda})\ ,$$
$$v^s(r)=\frac{e^2e^{-r/\lambda}}{r}\ . \tag{A6}$$

APPENDIX B

In this appendix we evaluate the term $T_0(l)/T_0(0)$. To do this we first evaluate the ring graph sum presented in Fig. 4(a):

$$\ln T_0(l)=\frac{\rho\beta^2}{2}\sum_{j=1}^{\infty}(-\beta\rho)^{j-1}\frac{(j-1)!}{j!}\int\cdots\int d\vec{r}_1\cdots d\vec{r}_j\,u(\vec{r}_{01},l)v(r_{12})\cdots v(r_{j-1,j})u(\vec{r}_{j0},l)\ . \tag{B1}$$

As in Appendix A, we make use of the Fourier transforms to write

$$\ln T_0(l)=\frac{\rho\beta^2}{2}\int\frac{d\vec{q}}{(2\pi)^3}u(\vec{q},l)u(-\vec{q},l)\epsilon^{-1}(q)\ . \tag{B2}$$

Since $T_0(0)$ simply requires $T_0(l=0)$, it follows that

$$\begin{aligned}\ln T_0(l)/T_0(0)&=\frac{\rho\beta^2}{2}\int\frac{d\vec{q}}{(2\pi)^3}\epsilon^{-1}(q)[u(\vec{q},l)u(-\vec{q},l)-u^2(q)]\\&=\frac{-\rho\beta^2}{2}\int\frac{d\vec{q}}{(2\pi)^3}\epsilon^{-1}(q)\left[\frac{\vec{l}\cdot\vec{q}}{e\beta}\right]^2u^2(q)\\&=\frac{-\alpha^3aL^2}{4(\alpha+1)^2}=-\gamma L^2\ ,\end{aligned} \tag{B3}$$

where in Eq. (B3)

$$L=l\epsilon_0;\quad a=r_0/\lambda;\quad \epsilon_0=e/r_0^2\ , \tag{B4}$$

and r_0 is the ion sphere radius defined by the expression

$$\frac{4\pi}{3}r_0^3\rho=1\ . \tag{B5}$$

[1]C. F. Hooper, Jr., Phys. Rev. 149, 177 (1966).
[2]J. E. Mayer, J. Chem. Phys. 18, 1426 (1950); E. Meeron, *ibid.* 18, 630 (1958); H. L. Friedman, *Ionic Solution Theory* (Interscience, New York, 1962).
[3]J. E. Mayer and M. G. Mayer, *Statistical Mechanics* (Wiley, New York, 1940).
[4]B. Mozer and M. Baranger, Phys. Rev. 115, 521 (1959).
[5]A. A. Broyles, Phys. Rev. 100, 1181 (1955).
[6]E. E. Salpeter, Ann. Phys. 5, 183 (1958).
[7]C. F. Hooper, Jr., Phys. Rev. 165, 215 (1968).
[8]R. J. Tighe and C. F. Hooper, Jr., Phys. Rev. A 15, 1773 (1977).
[9]H. Cramer, *Mathematical Methods of Statistics* (Princeton University, Princeton, N. J., 1957), p. 211.
[10]W. J. Swiatecki, Proc. R. Soc. (London) A205, 238 (1951).
[11]The Bateman Manuscript Project, *Higher Transcendental Functions*, edited by A. Erdélyi (California Institute of Technology, Pasadena, California, 1953), Vol. II, Chap. VII.
[12]H. Dewitt (private communication).
[13]J. C. Weisheit and E. L. Pollock, *Spectral Line Shapes*, edited by B. Wende (Walter de Gruyter, Berlin, 1981).
[14]B. Held and C. Deutsch, Phys. Rev. A 24, 540 (1981). This reference contains a comparison of the schemes in Refs. 1 and 4 and shows increasing disagreement as the value of a increases from 0.8 to 1.4. Therefore, it is safe to assume that the two methods will not agree at the larger $a=1.73$ value.
[15]Many authors have discussed this problem. Here we give a few: D. L. Bowers and E. E. Salpeter, Phys. Rev. 119, 1180 (1960); H. E. DeWitt *ibid.* 140A, 466 (1965); F. del Rio and H. E. DeWitt, Phys. Fluids 17, 791 (1969).